Available online at www.sciencedirect.com
SCIENCE DIRECT®
Surface Science 577 (2005) 1–14
SURFACE SCIENCE
www.elsevier.com/locate/susc

Kinetics of ammonia oxidation on stepped platinum surfaces. I. Experimental results

A. Scheibe, U. Lins, R. Imbihl *

Institut für Physikalische Chemie und Elektrochemie, Universität Hannover, Callinstr. 3-3a, 30167 Hannover, Germany

Received 12 October 2004; accepted for publication 14 December 2004
Available online 13 January 2005

Abstract

The kinetics of ammonia oxidation with oxygen have been investigated in the 10^{-5} and 10^{-4} mbar range on Pt(533) and Pt(443). Only N_2 and NO but no N_2O were detected as reaction products. The dependence of product formation on temperature and on the partial pressures of the reactants has been studied under steady state conditions. The reactive sticking coefficients were determined under reaction conditions with s_{reac} of ammonia reaching nearly 0.2. The Pt(533) surface was found to be catalytically more active than Pt(443) by a factor of 2–4.

Keywords: Platinum; Stepped platinum surface; Ammonia oxidation; Kinetics

1. Introduction

Catalytic ammonia oxidation with oxygen over platinum catalysts is an important process in the industrial production of nitric acid and in environmental catalysis [1]. Nitric acid is produced via formation of NO at $T > 800$ K in the so-called Ostwald process

$$4NH_3 + 5O_2 \rightarrow 4NO + 6H_2O,\ \Delta H = -226\ \text{kJ/mol} \quad \text{(R1)}$$

At lower temperature N_2 is the preferred reaction product

$$4NH_3 + 3O_2 \rightarrow 2N_2 + 6H_2O,\ \Delta H = -317\ \text{kJ/mol} \quad \text{(R2)}$$

In view of its industrial importance, comparatively few kinetic and mechanistic studies of catalytic ammonia oxidation have been made and only a relatively small number of single crystal investigations have been conducted [2–15]. A principle problem exists in extrapolating these single

* Corresponding author. Tel.: +49 5117622349; fax: +49 5117624009.
E-mail address: imbihl@pci.uni-hannover.de (R. Imbihl).

0039-6028/$ - see front matter © 2005 Elsevier B.V. All rights reserved.
doi:10.1016/j.susc.2004.12.027

crystal results to industrial conditions since the Pt catalysts undergo severe morphological changes due to the strong exothermicity of the reaction. A Pt/Rh gauze used in the Ostwald process becomes already visibly roughened during the first minutes of operation [16–18]. The restructuring of a catalyst under reaction conditions is a quite general phenomenon in heterogeneous catalysis often associated with an activation or deactivation of the catalyst [5,16–20]. The reaction-induced substrate changes are part of the well known pressure and material gap problem in catalytic research and catalytic ammonia oxidation is certainly an excellent example for this gap. A pressure gap also shows up in the product formation because in all studies N_2O formation according to

$$4NH_3 + 4O_2 \rightarrow 2N_2O + 6H_2O \qquad (R3)$$

was only detected at high pressure ($p > 1$ mbar).

In order to perform a systematic study of the effect of reaction-induced restructuring and its effect on the kinetics we chose two stepped Pt(1 1 1) surfaces, Pt(5 3 3) and Pt(4 4 3), as model systems for UHV studies under low pressure conditions ($p < 10^{-3}$ mbar). The Pt(5 3 3) surface written in microfacet notation as $4(1\,1\,1)\times 1(1\,0\,0)$ exhibits mono-atomic steps with (1 0 0) orientation while Pt(4 4 3) decomposed into $7(1\,1\,1)\times 1(1\,1\,1)$ contains mono-atomic steps with (1 1 1) orientation. Oxygen adsorption and NO decomposition, which both are mechanistic steps of the overall process, are known to be highly structure sensitive on Pt surfaces [21–24]. For this reason one would expect that the step orientation, the step density, and a change of the step structure by the reaction has a profound influence on the activity and selectivity of the catalyst. In catalytic CO oxidation on Pt(1 1 0) it was demonstrated that even very mild reaction conditions in the 10^{-4} mbar range can cause a roughening or (micro)facetting of the surface [25,26].

Single crystal studies of the $NH_3 + O_2$ reaction have been conducted with the orientations Pt(1 0 0) [13,14], Pt(1 1 1) [10–12], and Pt(s)-$12(1\,1\,1)\times(1\,1\,1)$ [9]. From the study of the stepped Pt(1 1 1) surface Gland and Korchak concluded that steps play a dominant role in determining the reactivity of the surface and that the availability of oxygen controls the selectivity towards NO formation in the competition N_2 vs NO formation [9]. In a molecular beam study Somorjai et al. found that NO production on Pt(1 1 1) occurs via a fast and a slow pathway associated with activation energies 121 ± 13 kJ/mol and 59 ± 13 kJ/mol, respectively [10]. With vibrational spectroscopy Michev and Ho identified on Pt(1 1 1) the intermediates OH, NH, and NH_2 [12]. The group of King studied the reaction on Pt(1 0 0) with a molecular beam and with vibrational spectroscopy [13,14]. The main conclusion from these studies was that direct ammonia dissociation according to $NH_{3,ad} \rightarrow N_{ad} + 3H_{ad}$ plays only a minor role in the overall activity. The main contribution comes from ammonia being activated through direct interaction with atomic oxygen or OH stripping one or several H atoms from the molecule. This conclusion is also supported by theoretical calculations [27]. A mechanistic scheme originally suggested by Fogel involved NO formation as primary step but this scheme found no support by experiments [3,14,15].

Here, we study in detail the kinetics of the reaction on the two surfaces under low pressure conditions, where mass transport limitations play no role and where the reaction is truly isothermal. As reported before, already under low pressure conditions the surface undergoes restructuring under certain reaction conditions associated with a change in selectivity [15]. Qualitatively, the results can be understood in terms of a simple mechanistic model. The interpretations are bolstered by simulations with a realistic mathematical model, which reproduces the main experimental results [28].

2. Experimental

The reaction was studied here in a standard UHV system equipped with LEED, a retarding field analyzer for Auger electron spectroscopy, a scanning tunneling microscope (DME), and a differentially pumped quadrupole mass spectrometer (QMS) for rate measurements. The base pressure in the UHV system was 2×10^{-10} mbar. The samples were heated indirectly by a filament behind the backside of the crystal either via radiation or

via electron bombardment. They were both prepared by repeated cycles of Ar-ion-sputtering, heating in oxygen ($p_{O_2} = 1 \times 10^{-6}$ mbar), followed by annealing to 1300 K. Gases of purity 5.0 for oxygen and 2.5 for ammonia were used. All pressures given here are uncorrected.

During rate measurements the cone (opening 2 mm), which connected the differentially pumped QMS with the main chamber, was brought 1 mm in front of the surface. In this way reaction products from the backside of the sample and from filaments were excluded. NO formation was followed in QMS via $m/e = 30$, N_2 via $m/e = 28$. The CO contribution to the mass 28 signal was determined from the $m/e = 12$ signal originating from CO fragmentation and then subtracted. The background was taken from rate measurements at 300 K assuming that the catalytic activity at this temperature is negligible. In order to determine the absolute reaction rates the QMS was calibrated against the ionization gauge in the main chamber.

3. Results

3.1. Temperature dependence of the kinetics

Structural models of the Pt(533) and Pt(443) surfaces are displayed in Fig. 1, together with a characterization of the surfaces by LEED and scanning tunneling microscopy. The temperature

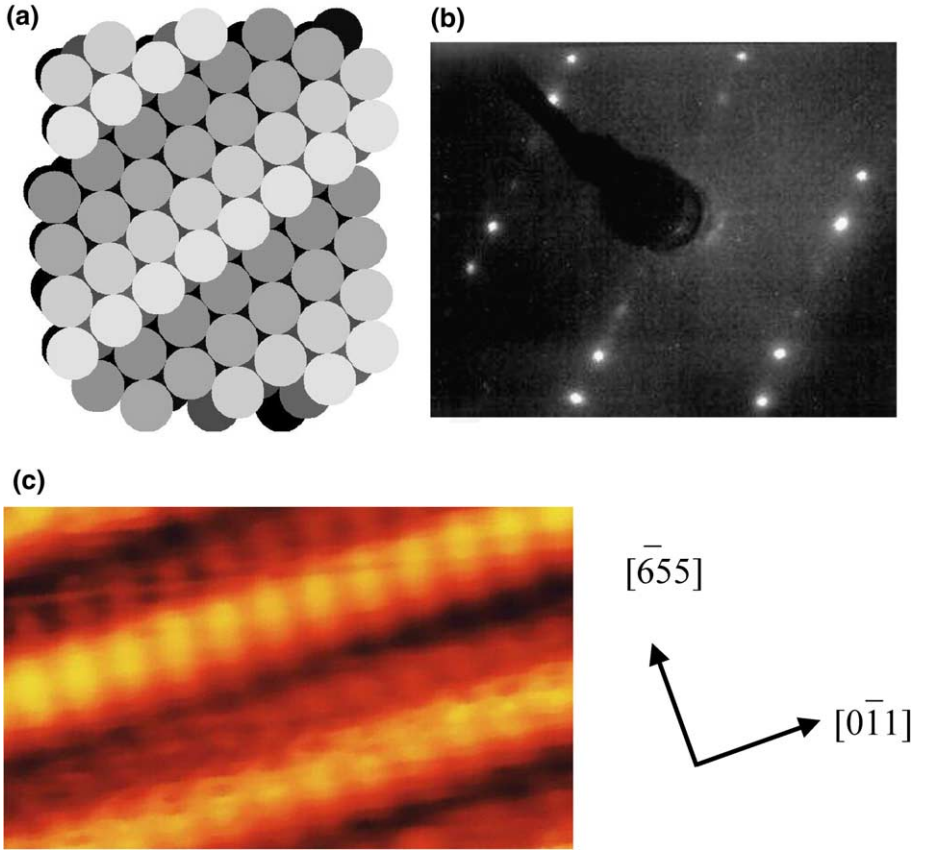

Fig. 1. Structural models of the stepped Pt(111) surfaces used in this investigation together with a characterization by scanning tunneling microscopy (STM) and LEED. (a) Structural model of Pt(533) surface, (b) LEED pattern of Pt(533), (c) STM image of Pt(533), (d) model of Pt(443) surface, (e) LEED pattern of Pt(443), (f) STM image of Pt(443).

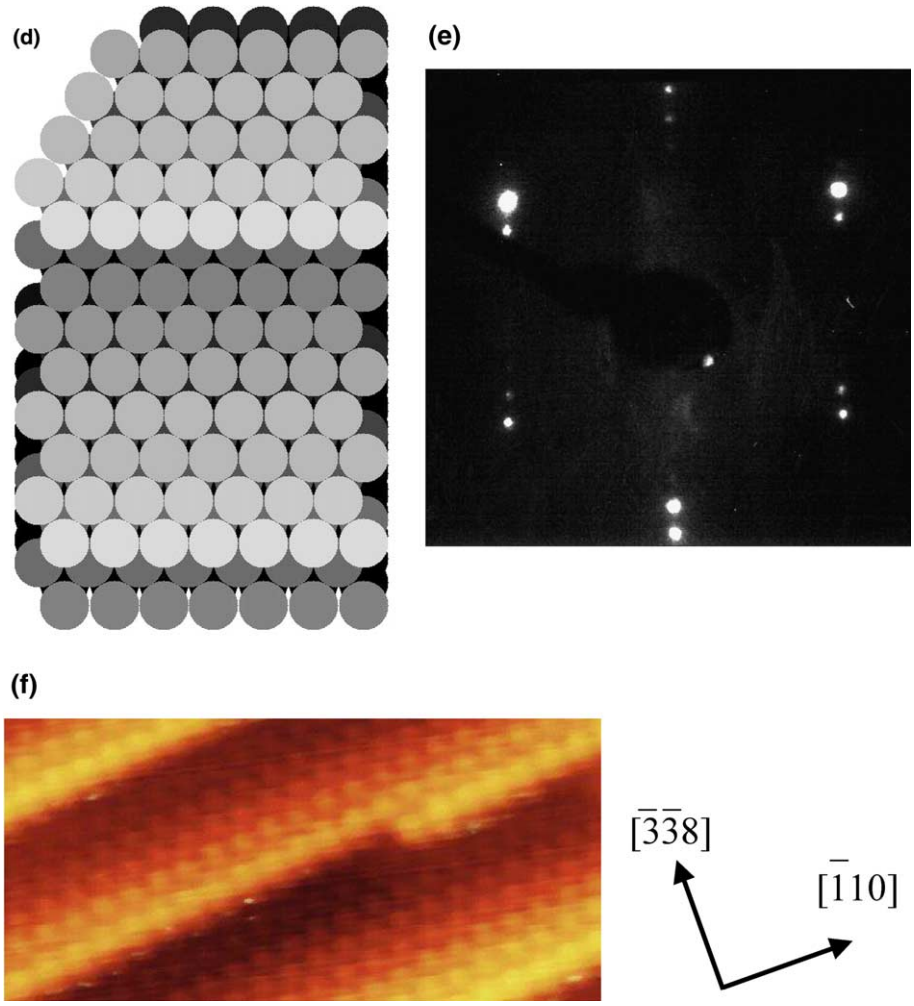

Fig. 1 (*continued*)

dependence of the NO and N_2 production rates of Pt(5 3 3) and Pt(4 4 3) are reproduced in Figs. 2 and 3 for different partial pressure ratios p_{O_2}/p_{NH_3} of oxygen to ammonia. The data were obtained by slowly cycling the temperature with fixed p_{O_2} and p_{NH_3}, starting always with a freshly prepared surface. The qualitative picture is similar irrespective of orientation and partial pressure ratio. N_2 production is the preferred reaction channel at low temperature but, with increasing temperature, NO formation is favored, while N_2 production drops to a low level.

On Pt(5 3 3) quite large hysteresis effects are observed while on Pt(4 4 3) the hystereses are generally small and they are probably transients, i.e. they tend to vanish if the heating/cooling rate is chosen sufficiently slow. As was demonstrated by LEED and STM, the large hystereses on Pt(5 3 3) have their origin in a reaction-induced doubling of the step height and terrace width, which occurs on the heating branch of a cycle [15]. The N_2 rate curve exhibits a dip when the surface restructures. The hysteresis before this dip appears not to be a true hysteresis because it vanishes when the heating/cooling is carried out sufficiently slow. Under reaction conditions this doubling of the step height is reversible and above ≈650–750 K single atomic steps are restored as indicated in the bars on top

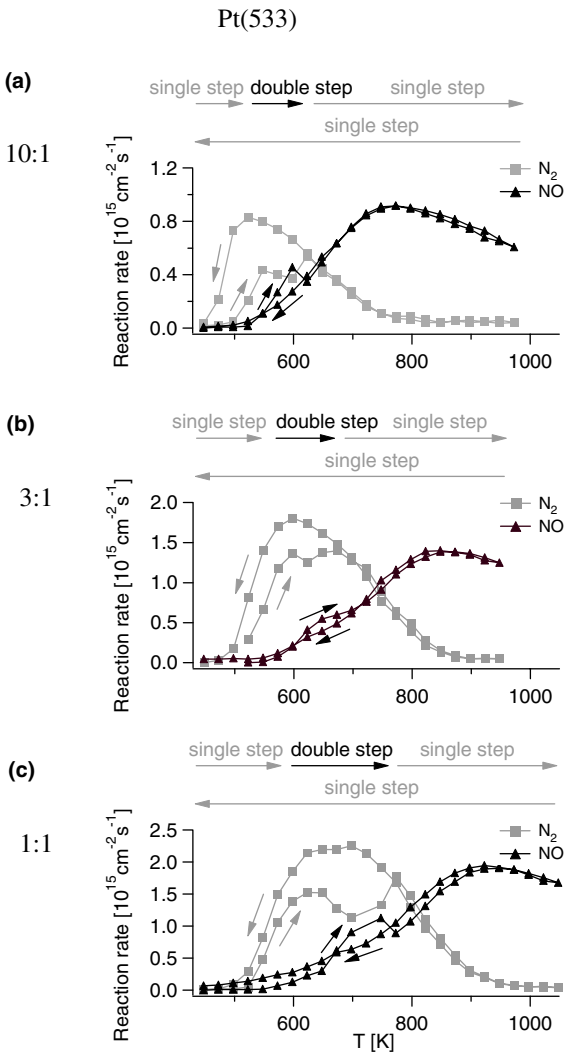

Fig. 2. Temperature dependence of the N_2 and NO production rates on Pt(533) at varying mixing ratios p_{O_2}/p_{NH_3} with fixed $p_{O_2} = 1 \times 10^{-4}$ mbar. The arrows indicate that the rates were measured in heating/cooling cycles with 50 K/min starting in each case with a freshly prepared surface. The error bars are indicated by the size of the symbols used for representing the data points. This applies also to all other figures unless the error bars are explicitly given. The bar on top of each diagram shows the structural changes of the surface as determined by LEED.

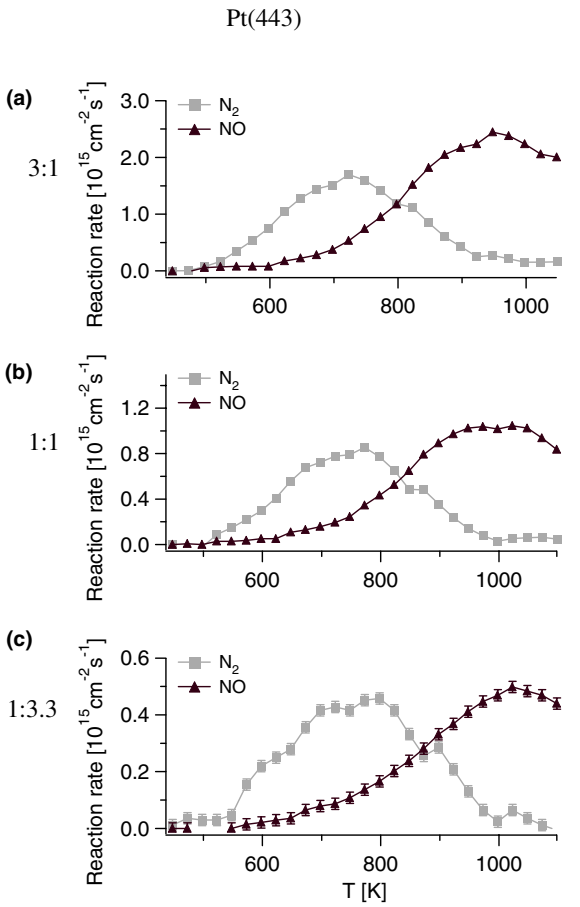

Fig. 3. Temperature dependence of the N_2 and NO production rates on Pt(443) at varying mixing ratios p_{O_2}/p_{NH_3} with fixed $p_{NH_3} = 1 \times 10^{-4}$ mbar. A heating rate of 100 K/min was applied. Error bars, cf. caption of Fig. 2.

of the diagrams in Fig. 2. On the cooling branch the steps remain single atomic. This doubling in step height, which, at higher temperature $T \geqslant 1100$ K can also be induced by oxygen alone, is associated with a significant change in selectivity towards enhanced NO production [15,29]. The reaction-induced doubling of the step height was not observed at $p < 10^{-5}$ mbar, indicating that a certain threshold in pressure exists for such structural changes to occur under reaction conditions. This is demonstrated in Fig. 4, where a large hysteresis is observed at a total pressure of 2×10^{-4} mbar. The hysteresis, however, becomes much smaller when the total pressure is reduced to 6×10^{-5} mbar. On Pt(443) no reaction-induced structural changes were detectable in the pressure range from 10^{-6} to 10^{-3} mbar with LEED.

We note in Fig. 2 that the rate maxima for both, N_2 and NO, shift with increasing ratio p_{O_2}/p_{NH_3} to

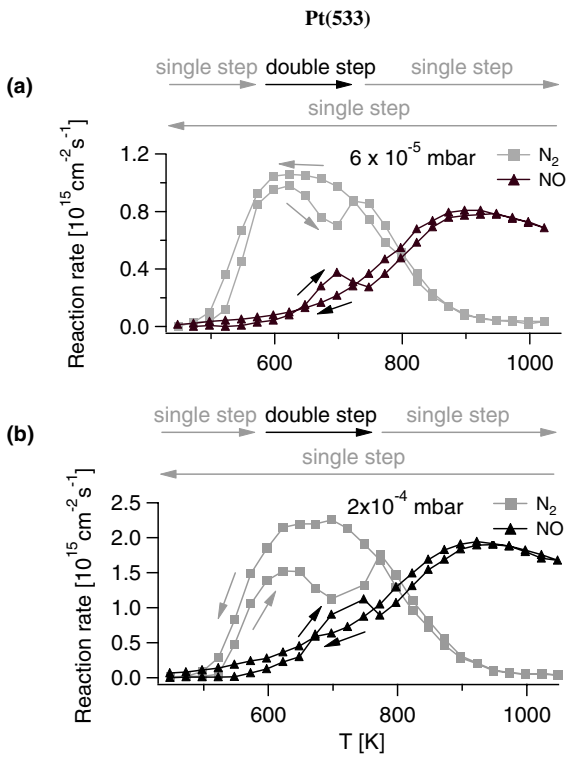

Fig. 4. Influence of the total pressure on the width and the amplitude of the hysteresis that arises during a heating/cooling cycle on Pt(533) with a mixing ratios p_{O_2}/p_{NH_3} of 1:1. The bars on top of each figure demonstrate the structural changes as verified by LEED. A heating rate of 100 K/min was used. Error bars, cf. caption of Fig. 2. (a) $p_{total} = 6 \times 10^{-5}$ mbar, (b) $p_{total} = 2 \times 10^{-4}$ mbar.

lower temperature, i.e. in the case of nitrogen from about 670 K for a 1:1 ratio to 530 K as the ratio is increased to 10:1. For NO production the corresponding shift is nearly the same. Furthermore, the width of the N_2 peak narrows considerably with increasing excess of oxygen from about 400 K at a 1:1 ratio to roughly 250 K at 10:1. With increasing p_{O_2}/p_{NH_3} also the region of reaction-induced restructuring shifts to lower temperature as reflected by the shift in the dip of the N_2 rate curves.

The comparison of the absolute rates shows that, depending on the ratio p_{O_2}/p_{NH_3}, the Pt(533) orientation is catalytically more active than Pt(443) by a factor 2 to 4. The rate maxima of N_2/NO production appear at higher temperature on Pt(443) as compared to Pt(533) by approximately 100–140 K in the case of N_2 production and by 50–80 K in the case of NO production. We also note that similar to Pt(533) all rate maxima shift with decreasing ratio p_{O_2}/p_{NH_3} to higher temperature but the shift is much smaller, reaching only 30 K in the case of nitrogen and 50 K for NO production.

3.2. Reactive sticking coefficients

In our experimental set-up the differentially pumped QMS is behind a cone whose tip is about 1–2 mm's away from the sample surface. Due to this geometric arrangement to a good approximation only molecules reflected from the surface can enter the cone to be detected by the QMS: We can thus determine the reactive sticking coefficient s_{reac} in situ from the measured variation of the reactant partial pressures, i.e. of O_2 or NH_3. Denoting the signal of a gas without reaction by I_0 and during reaction with I we calculate the reactive sticking coefficient s_{reac} as

$$s_{reac} = \frac{I_0 - I}{I_0}$$

In our case we take the signal at 300 K for I_0, assuming a negligible reaction rate at this temperature.

Fig. 5 displays a comparison of the reactive sticking coefficients for both surfaces and both gases measured under the steady state conditions of a temperature cycling experiment. Under steady state conditions the number of atoms which adsorb and react, has to be equal to the sum of the atoms in the products which leave the surface. The number of nitrogen atoms adsorbing has to be equal to the number of N atoms in the products leaving the surface and the corresponding amount of oxygen depends on the relative contributions of the two pathways given by (R1) and (R2). We have

$$\begin{aligned} 4s_{reac}(NH_3)\lambda_{NH_3}p_{NH_3} &= 4r_{NO} + 2r_{N_2} \\ &= Ps_{reac}(O_2)\lambda_{O_2}p_{O_2} \end{aligned}$$

where λ_i is the impingement rate of the gas i per 1 cm^2 surface area according to kinetic gas theory, i.e.

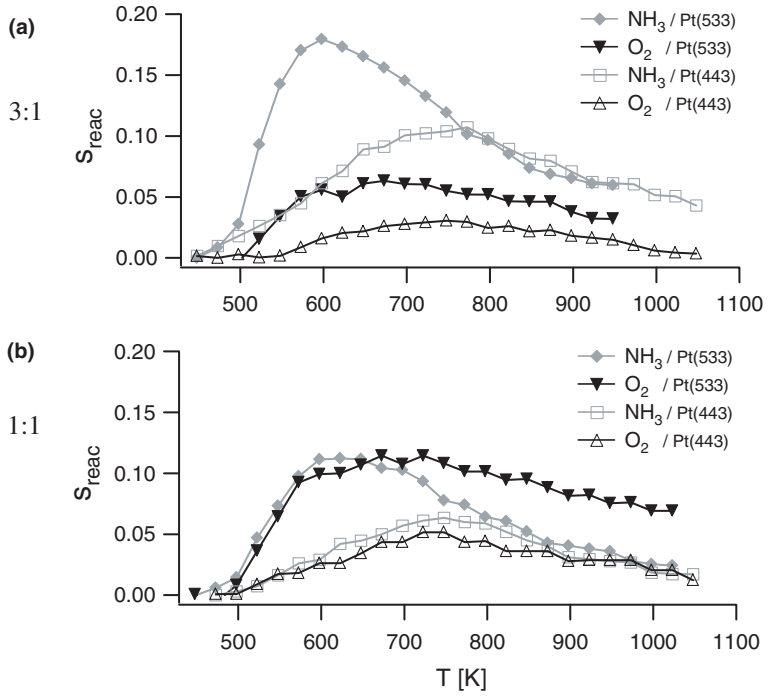

Fig. 5. Comparison of the reactive sticking coefficients, s_{reac}, of the reacting gases on Pt(533) and Pt(443) for different mixing ratios. The ammonia partial pressure was kept fixed at $p_{NH_3} = 3 \times 10^{-5}$ mbar in all experiments. The data shown were obtained from the heating part of a heating/cooling cycle with a heating rate of 100 K/min. Error bars, cf. caption of Fig. 2. (a) $p_{O_2} = 1 \times 10^{-4}$ mbar, (b) $p_{O_2} = 3 \times 10^{-5}$ mbar.

$$\lambda_i = \frac{p_i}{\sqrt{2\pi m_i kT}}$$

and P denotes a stoichiometric factor according to the different O_2/NH_3 ratios in the two reaction channels, described by reaction equations (R1) and (R2). P is given by

$$P = \frac{2(5r_{NO} + 3r_{N_2})}{r_{NO} + r_{N_2}}$$

With the above expression we can check whether mass conservation is fulfilled and this is the case for the data in Fig. 5, together with the corresponding reaction rates. The data demonstrate that the reactive sticking coefficient for ammonia can be quite high if oxygen is in excess, reaching nearly 0.2 in the N_2 rate maximum of Pt(533). The reactive sticking coefficient for oxygen is highest when ammonia is in excess going up to 0.12 on Pt(533) and 0.05 on Pt(443). Due to a higher step density on Pt(533), which is 1/4 as compared to the 1/7 of Pt(443) (cf. Fig. 1), one would expect a higher oxygen sticking coefficient on Pt(533). This is what we see but the ratio of 2.4 is larger than the ratio of the step densities, which only amounts to 7/4 = 1.75. We should keep in mind that the reactive sticking coefficient is only a lower boundary for the total sticking coefficient s, i.e. we always have $s > s_{reac}$ since particles adsorbing with the sticking probability s may either react or desorb without reaction.

With increasing temperature the reactivity of the surface decreases beyond 600–700 K, as reflected by a decreasing s_{reac} in Fig. 5. The surface residence time of ammonia becoming too small before reaction can occur will be one of the factors responsible for this decrease. The other factor is that on Pt(111) surfaces the oxygen sticking for dissociative chemisorption decreases with rising temperature as a consequence of the smaller population of the molecular precursor state for dissociation [22].

3.3. Dependence on partial pressure

The dependence of the kinetics of NO and N_2 production on the oxygen partial pressure at two temperatures, $T = 550$ K and $T = 625$ K, is displayed in Figs. 6–9 for Pt(5 3 3) and Pt(4 4 3), respectively. All data shown here were measured by stepwise increasing p_{O_2}, starting from zero. Hysteresis effects, which arise when the pressure is cycled due to reaction-induced structural changes, are thus absent in the diagrams [15]. We first discuss the results for Pt(5 3 3) in Figs. 6 and 7. The data in Fig. 6 for $T = 550$ K and $p_{NH_3} = 1 \times 10^{-5}$ mbar show that at low p_{O_2}, N_2 formation is the preferred reaction channel. With increasing p_{O_2} N_2 formation starts to level off while NO formation continues to rise. The saturation of the N_2 production with increasing p_{O_2} can only be seen up to $p_{NH_3} = 3 \times 10^{-5}$ mbar (not shown here), whereas in the 10^{-4} mbar range the required p_{O_2} lies beyond the experimentally accessible parameter range. At $p_{NH_3} = 1 \times 10^{-5}$ mbar in Fig. 6a the reaction order (RO) for N_2 and NO production

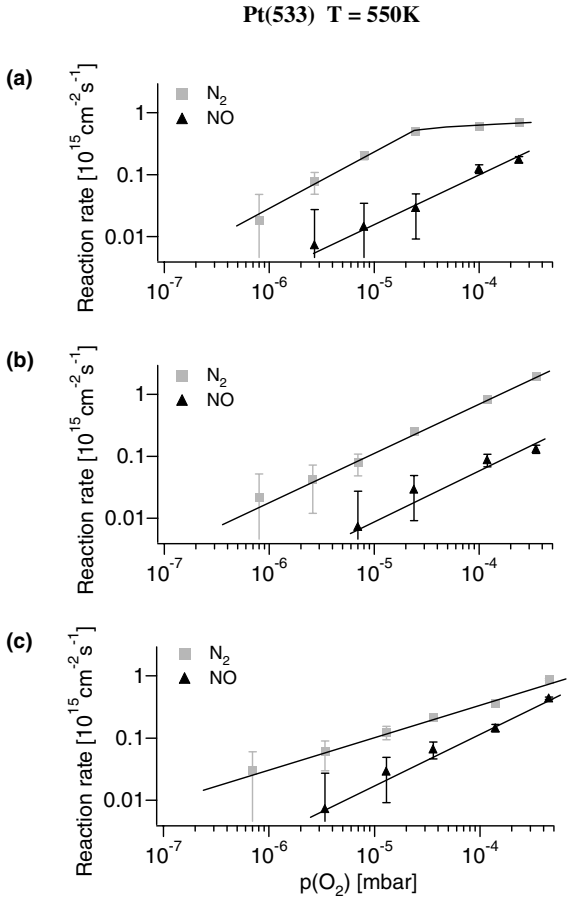

Fig. 6. Dependence of the N_2 and NO production rates of Pt(5 3 3) on p_{O_2} at $T = 550$ K. The data were measured by stepwise increasing p_{O_2} starting from zero. The lines connecting the experimental data points have been drawn to guide the eye. (a) $p_{NH_3} = 1 \times 10^{-5}$ mbar, (b) $p_{NH_3} = 1 \times 10^{-4}$ mbar, (c) $p_{NH_3} = 3 \times 10^{-4}$ mbar.

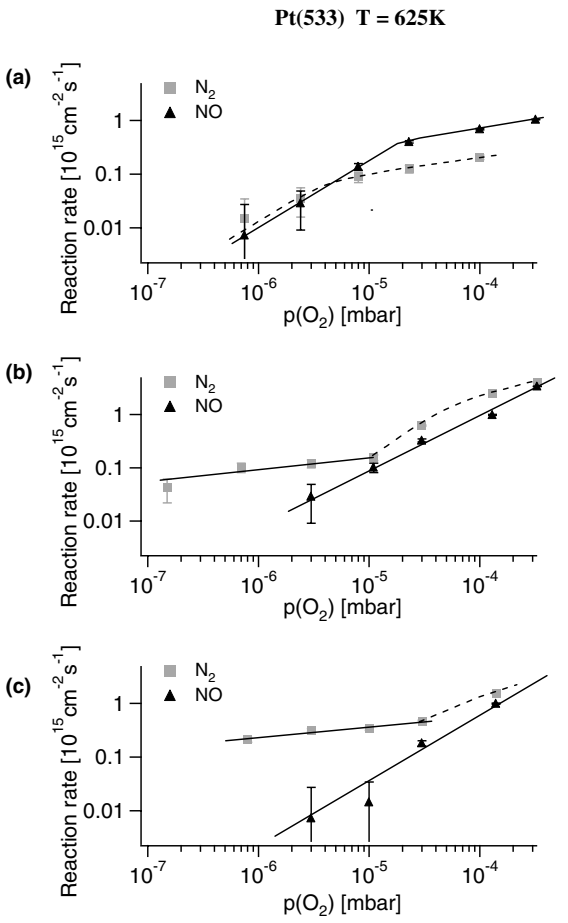

Fig. 7. Dependence of the N_2 and NO production rates of Pt(5 3 3) on p_{O_2} at $T = 625$ K. Data were measured by stepwise increasing p_{O_2}. The lines connecting the experimental data points have been drawn to guide the eye. (a) $p_{NH_3} = 1 \times 10^{-5}$ mbar, (b) $p_{NH_3} = 1 \times 10^{-4}$ mbar, (c) $p_{NH_3} = 3 \times 10^{-4}$ mbar.

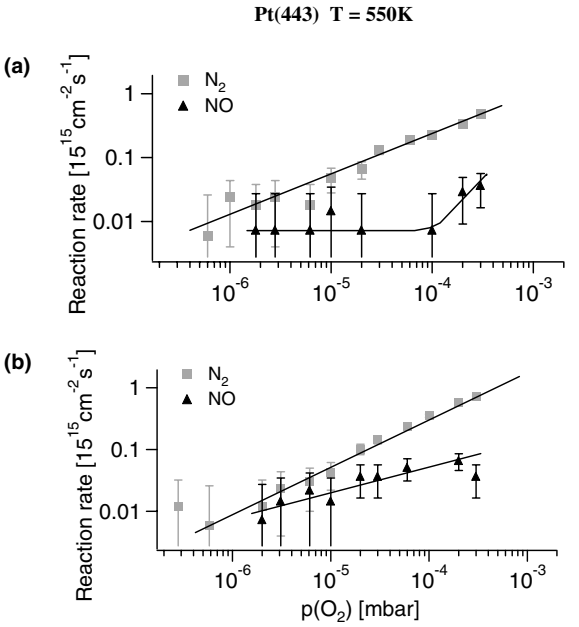

Fig. 8. Dependence of the N_2 and NO production rates of Pt(443) on p_{O_2} at $T = 550$ K. Data were measured by stepwise increasing p_{O_2}. The lines connecting the experimental data points have been drawn to guide the eye. (a) $p_{NH_3} = 1 \times 10^{-5}$ mbar, (b) $p_{NH_3} = 1 \times 10^{-4}$ mbar.

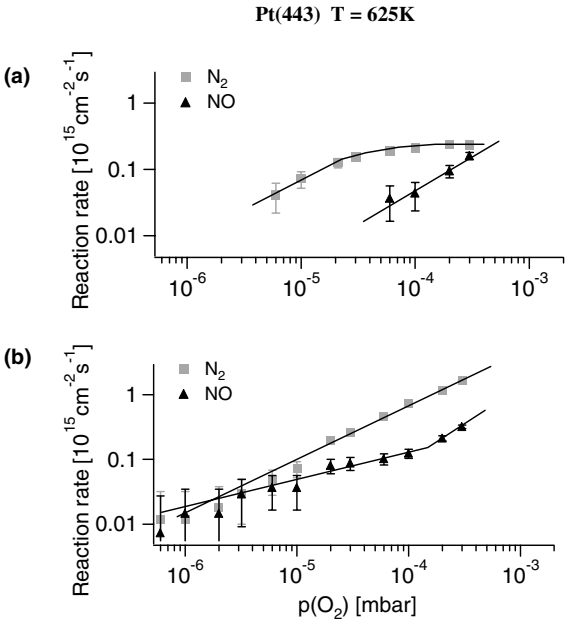

Fig. 9. Dependence of the N_2 and NO production rates of Pt(443) on p_{O_2} at $T = 625$ K. Data were measured by stepwise increasing p_{O_2}. The lines connecting the experimental data points have been drawn to guide the eye. (a) $p_{NH_3} = 1 \times 10^{-5}$ mbar, (b) $p_{NH_3} = 1 \times 10^{-4}$ mbar.

is 0.8 and 0.7, respectively. Increasing p_{NH_3} to 1×10^{-4} mbar decreases the RO for N_2 to 0.7 so that both products have the same RO of 0.7. A further increase of p_{NH_3} to 3×10^{-4} mbar leaves the RO for NO unchanged but the RO for N_2 drops to 0.3, as shown by Fig. 6c.

At $T = 625$ K with oxygen being in excess, one has reaction conditions close to the N_2 rate maximum in Fig. 2. The corresponding dependence of the rates on p_{O_2} is displayed in Fig. 7. With $p_{NH_3} = 1 \times 10^{-5}$ mbar the NO and N_2 production increase both initially with a RO close to unity, as demonstrated by Fig. 7a. Beyond $p_{O_2} = 2 \times 10^{-5}$ mbar the rates level off and increase only slightly with p_{O_2}. Increasing p_{NH_3} in the 10^{-4} mbar range we can distinguish two different regimes in N_2 production, as evidenced by Fig. 7b. Below $p_{O_2}/p_{NH_3} = 1{:}10$, with ammonia being strongly in excess, the N_2 production increases weakly with p_{O_2}, yielding a RO of 0.2. Above the 1:10 ratio the RO jumps to one. The RO order for NO formation is always close to one at $T = 625$ K irrespective of p_{NH_3}. We can attribute the low RO order for N_2 formation below $p_{O_2}/p_{NH_3} = 1{:}10$ to the presence of a large ammonia coverage on the surface inhibiting O_2 adsorption. The inhibition restricts the reaction to a few reactive centers, i.e. surface defects, where ammonia cannot block adsorption sites.

The corresponding data for Pt(443) measured at the same temperatures of 550 K and 625 K are displayed in Figs. 8 and 9. With respect to the position relative to the production maxima the conditions are different from Pt(533), as shown by Fig. 3. On Pt(443) the rate maximum for N_2 production lies about 100 K higher in temperature than on Pt(533). We therefore expect no saturation of N_2 production upon increasing p_{O_2} and the NO production should be quite low, unless we go to very high p_{O_2}. This is more or less what we observe in Figs. 8 and 9. At $p_{NH_3} = 1 \times 10^{-5}$ mbar in Fig. 8a the N_2 production exhibits a RO of 0.4 with respect to oxygen. NO formation sets in notably only beyond $p_{O_2}/p_{NH_3} = 1{:}10$, increasing then

steeply with RO ≈ 1. Raising p_{NH_3} to 1×10^{-4} mbar increases the RO for N_2 to 0.6, whereas the RO for NO formation decreases to 0.25, as demonstrated by Fig. 8b.

At higher temperature, at $T = 625$ K, the N_2 formation saturates with increasing p_{O_2}, as shown in Fig. 9a for $p_{NH_3} = 1 \times 10^{-4}$ mbar. NO production becomes significant only beyond a 10:1 ratio exhibiting 1st order kinetics with respect to oxygen. As shown by Fig. 9b, raising p_{NH_3} to 1×10^{-4} mbar changes the RO for N_2 production to 0.7 in the investigated parameter range. NO production obeys a kinetics with RO = 0.3 under conditions of ammonia being in excess.

The dependence of the reaction kinetics of Pt(533) on the ammonia partial pressure is displayed in Fig. 10 for $T = 525$ K and $T = 625$ K. Experimentally it is difficult to extend the parameter range to very low p_{NH_3} due to saturation of the walls with NH_3. At $T = 625$ K in Fig. 10a the N_2 production saturates quite early below a 10:1 ratio p_{O_2}/p_{NH_3}. The NO kinetics exhibits a quite unusual behavior because above $p_{NH_3} = 1 \times 10^{-5}$ mbar the rate of NO formation increases with p_{NH_3}, whereas the opposite tendency is expected. The effect is reproducible and could so far not been traced back to an artefact like reaction at hot filaments. At $T = 625$ K the formation of N_2 and NO increases initially with p_{NH_3} and then both rates saturate quite early.

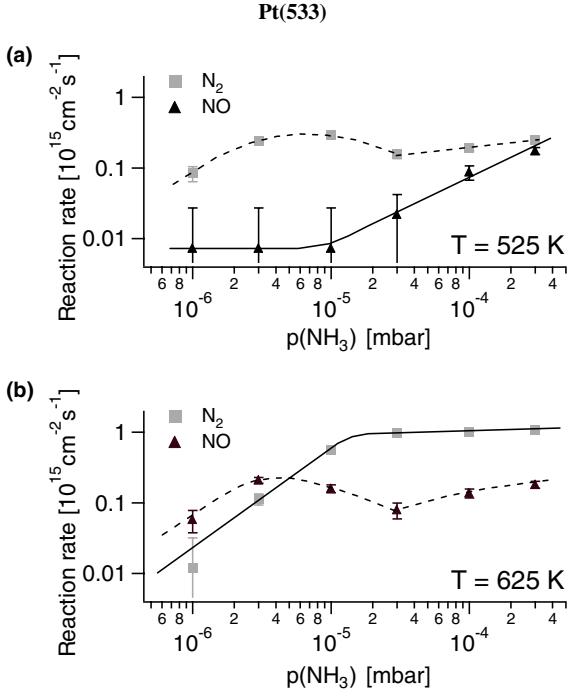

Fig. 10. Dependence of the N_2 and NO production rates of Pt(533) on p_{NH_3} at fixed $p_{O_2} = 3 \times 10^{-5}$ mbar. Data were measured by stepwise increasing p_{NH_3}. The lines connecting the experimental data points have been drawn to guide the eye. (a) $T = 525$ K, (b) $T = 625$ K.

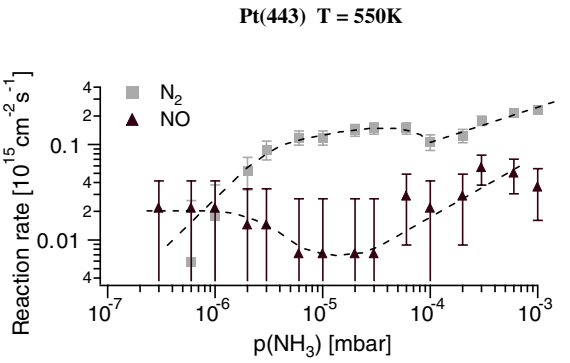

Fig. 11. Dependence of the N_2 and NO production rates of Pt(443) at $T = 550$ K on p_{NH_3} at fixed $p_{O_2} = 1 \times 10^{-5}$ mbar. Data measured by stepwise increasing p_{NH_3}. The lines connecting the experimental data points have been drawn to guide the eye.

On Pt(443) we obtain a quite similar behavior as on Pt(533), as demonstrated in Fig. 11 for $T = 550$ K. Over a broad parameter range both production rates exhibit a zeroth order kinetics with respect to p_{NH_3}, except that at high p_{NH_3} the NO production starts to increase with p_{NH_3}. Just the opposite effect should be expected from the surface chemistry but the effect turned out to be reproducible.

4. Discussion

While operating conditions in the Ostwald process have been optimized a long time ago achieving high conversions, comparatively few kinetic and mechanistic studies with the $NH_3 + O_2$ reaction on platinum have been published. The kinetics of the $NH_3 + O_2$ reaction on polycrystalline Pt, Rh,

and Ir wires have been measured in the p range 0.1–1 mbar by Pignet and Schmidt [4]. On supported catalysts the variation of the catalytic activity with Pt loading was attributed to particle size effects [7]. The kinetics of the reaction in a microreactor with supported Pt as catalyst have been investigated by Rebrov et al. [8]. With positron emission profiling Sobczyk et al. succeeded in following the distribution of isotope labeled species in a reactor with a resolution of 3 mm [30].

The dynamics of the $NH_3 + O_2$ reaction on Pt have been investigated by several groups in the mbar—1 atm pressure range. Rate oscillations and stationary and non-stationary *T*-patterns on electrically heated Pt wires and ribbons have been reported [31–34]. Hysteresis effects, in connection with ignition/extinction phenomena, were demonstrated by Barelko and Volodin [5]. All these phenomena appear to be limited to the use of high pressures ($p > 1$ mbar) because so far no such phenomena have been reported in low pressure single crystal studies.

At higher pressure mass transport and not surface chemistry will limit the conversion rates because of the high catalytic activity of the Pt surface. The high activity is also corroborated by our results, showing that the reactive sticking coefficient for ammonia can reach 0.2 (cf. Fig. 5). In low pressure single crystal studies such transport limitations are absent.

According to recent studies the dissociation of ammonia according to

$$NH_{3,ad} \rightarrow N_{ad} + 3H_{ad} \quad \text{(R4)}$$

contributes little to the overall activity [13]. Direct hydrogen abstraction by chemisorbed oxygen or OH species is the dominant reaction pathway for product formation. With the asterisk * denoting a vacant adsorption site the reaction mechanism in simplified form can be formulated as

$$O_2 + 2* \Longleftrightarrow 2O_{ad} \quad \text{(R5)}$$

$$NH_3 + * \Longleftrightarrow NH_{3,ad} \quad \text{(R6)}$$

$$NH_{3,ad} + O_{ad} \Longleftrightarrow NH_{2,ad} + OH_{ad} \quad \text{(R7)}$$

$$NH_{2,ad} + O_{ad} \Longleftrightarrow NH_{ad} + OH_{ad} \quad \text{(R8)}$$

$$NH_{ad} + O_{ad} \Longleftrightarrow N_{ad} + OH_{ad} \quad \text{(R9)}$$

$$NH_{3,ad} + OH_{ad} \rightarrow NH_{2,ad} + H_2O + * \quad \text{(R10)}$$

$$NH_{2,ad} + OH_{ad} \rightarrow NH_{ad} + H_2O + * \quad \text{(R11)}$$

$$NH_{ad} + OH_{ad} \rightarrow N_{ad} + H_2O + * \quad \text{(R12)}$$

$$2N_{ad} \rightarrow N_2 + 2* \quad \text{(R13)}$$

$$N_{ad} + O_{ad} \Longleftrightarrow NO_{ad} + * \quad \text{(R14)}$$

$$NO_{ad} \rightarrow NO + * \quad \text{(R15)}$$

$$O_{ad} + H_{ad} \Longleftrightarrow OH_{ad} \quad \text{(R16)}$$

$$OH_{ad} + H_{ad} \rightarrow H_2O + 2* \quad \text{(R17)}$$

$$2OH_{ad} \Longleftrightarrow O_{ad} + H_2O \quad \text{(R18)}$$

For N_2O formation, which was not observed at low p ($p < 10^{-3}$ mbar), two reaction pathways can be considered for N_2O, which should immediately desorb at $T > 300$ K:

$$NO_{ad} + O_{ad} \rightarrow N_2O + 2* \quad \text{(R19)}$$

$$2NO_{ad} \rightarrow N_2O + O_{ad} + * \quad \text{(R20)}$$

Quantum chemical calculations support the latter mechanism on Pt surfaces since it exhibits a lower activation barrier than step (R19) [35]. The reverse reaction to (R20) was shown to be dominant in N_2O decomposition over Pt [36].

The different regimes of the reaction can easily be summarized. The main factors controlling the NO formation are the availability of atomic oxygen and nitrogen and a high enough temperature so that NO can desorb. At lower temperature with a small oxygen coverage and a large amount $NH_X (X = 1–3)$ species N_2 formation will be dominant. At too low temperatures the reactivity of the surface tends towards zero, apparently as a consequence of a high adsorbate coverage inhibiting oxygen adsorption. At too high temperature the reactivity of the surface also becomes very small due to the residence time of NH_3 becoming too small for reaction and as a consequence of an oxygen sticking coefficient which decreases with

temperature [22]. Simulations with a realistic mathematical model based on the above scheme could reproduce the behavior of the single crystal qualitatively correct and to a large degree even quantitatively [28,37].

A molecular beam study of the $NH_3 + O_2$ reaction on Pt(1 0 0) yielded rather similar results as found here on Pt(5 3 3) [13]. With a NH_3/O_2 mixture containing 90% O_2 the rate maximum of N_2 production is found at 500 K while we observe the maximum at 520 K with a ratio 10:1 (cf. Fig. 2). For NO production we note a significant difference because the rate maximum on Pt(1 0 0) for a mixture with 90% O_2 lies around 600–700 K, whereas we find a rate maximum at 770 K for a 10:1 ratio (cf. Fig. 2). When we compare our data with those of Pignet and Schmidt for Pt wires we realize that their rate maxima lie at higher temperature as a consequence of the higher pressure of $p \approx 1$ mbar they use [4]. With a gas mixture with 40% NH_3 the rate maximum for N_2 lies at 620 K but for a mixture with 90% NH_3 the maximum shifts strongly to ≈1000 K. The corresponding numbers for NO production are 1050 K and ≈1300 K, respectively, for the two mixtures. The trend that the rate maxima with decreasing oxygen content of the gas mixture shift to higher temperature is the same as in our experiments (cf. Fig. 2).

The concept of using stepped surfaces as a model catalyst for structure sensitive reactions has been applied in quite a number of studies since the first investigations by Somorjai and coworkers [38]. The choice to use the two orientations Pt(5 3 3) and Pt(4 4 3) as model catalysts for the $NH_3 + O_2$ reaction on Pt was motivated by two facts. On one hand in the absence of reaction-induced restructuring the (1 1 1) orientation will be dominant on polycrystalline Pt for thermodynamic reasons, while on the other hand a flat Pt(1 1 1) surface is fairly unreactive due to the low sticking coefficient of oxygen [21,22].

Compared to Pt(4 4 3) the Pt(5 3 3) orientation is more active by a factor of 2–4, as judged from the height of the rate maxima. The higher step density of Pt(5 3 3) compared to Pt(4 4 3) already accounts for a factor of 7/4 = 1.75 but the remaining factor of 1.1–2.2 might be due to a higher catalytic activity of (1 0 0) steps compared to (1 1 1) steps, leaving aside the possibility that this factor might be within the experimental uncertainty. Both, dissociative oxygen chemisorption as well as NO decomposition are highly structure sensitive as is known from numerous studies with Pt single crystal surfaces [21–24]. In addition, it is also demonstrated that ammonia adsorption on platinum surfaces is structure sensitive with the sticking coefficient increasing on rough surfaces [39]. The sticking coefficient of ammonia on Pt(210) is about ten times higher on Pt(210) than on Pt(1 1 1) and for the dissociation probability the difference is even larger.

For oxygen adsorption the differences in the initial sticking coefficients are not known for the two surfaces since only data for $Pt(5\,3\,3)/O_2$ can be found in the literature [40]. If we assume that the reactive sticking coefficients displayed in Fig. 5 reflects this difference then we have roughly the same factor of 2 we already have from the step density. In temperature programmed desorption (TPD) experiments it was shown that about 60% of the initially molecularly adsorbed NO decomposes on Pt(1 0 0), whereas Pt(1 1 1) and Pt(1 1 0) exhibit a rather low dissociation probability [23,24,41]. The highest activity for NO decomposition was found on Pt(4 1 0). According to the principles of microscopic reversibility one would expect to find a similar trend also for the reverse process, i.e. NO formation via (R14). If we assume that (1 0 0) steps exhibit a particularly high activity in NO dissociation and hence NO association, this would explain the higher activity of Pt(5 3 3).

Our data in fact support a particular role of (1 0 0) steps because we observe a drastic change in selectivity from preferential N_2 formation to NO production as the single atomic steps on Pt(5 3 3) undergo a doubling in step height. Quantum chemical calculations show that the transition state for NO dissociation on Pt(1 0 0)-1×1 is a flat-lying NO molecule with the N atom and the O-atom bonded each to two Pt atoms of the four Pt atoms, forming the square of the (1×1) unit cell of the substrate [35]. One might speculate that this transition state on the (1 0 0) double steps of Pt(5 3 3) is energetically less affected by space interactions with surrounding adsorbate molecules than on the single atomic steps of the same surface.

The energetically more favorable transition state might explain why the restructuring leads to a preference towards NO formation.

On Pt(5 3 3) the doubling of the step height was shown to occur only at $p > 10^{-5}$ mbar in a temperature window of roughly 500–750 K [15,39]. On Pt(4 4 3) no structural changes were detectable in LEED after exposure to reaction conditions in the 10^{-5} and 10^{-4} mbar range [37]. With STM however, it was demonstrated that even adsorption of ammonia alone at 300 K leads to a step restructuring [37]. The originally straight step edges start to meander in the presence of adsorbed ammonia. Because the average step separation does not change the meandering does not show up in LEED by a different spot splitting. A step meandering under reaction conditions can thus not be excluded for Pt(4 4 3).

The morphological changes Pt undergoes in the $NH_3 + O_2$ reaction were studied systematically by Schmidt et al. using small single crystalline Pt spheres (<0.5 mm) as catalysts [16–18]. The conditions they used—atmospheric pressure and temperatures up to 1100 K—are, however, quite drastic compared to ours. Under these conditions, which are comparable to those of the Ostwald process, different mechanisms will be dominant in catalytic etching, like the formation of volatile Pt oxides.

5. Conclusions

It was shown that both stepped Pt(1 1 1) surfaces, Pt(5 3 3) and Pt(4 4 3), are catalytically very active in the $NH_3 + O_2$ reaction, as evidenced by the high values of the reactive sticking coefficients. Pt(5 3 3) is more active than Pt(4 4 3) by a factor of 2–4 what can be attributed to (i) the higher step density of Pt(5 3 3) and (ii) possibly to a higher activity of (1 0 0) step sites as compared to (1 1 1) step sites. The apparent reaction order of product formation varies strongly with the reaction conditions. What this study also demonstrates is that reaction-induced structural changes are also occurring under quite mild reaction conditions and that these changes affect the activity and selectivity of the $NH_3 + O_2$ reaction.

Acknowledgment

This work was supported by the DFG under the priority program 1091 ‘‘Bridging the gap between ideal and real systems in heterogeneous catalysis’’.

References

[1] T.H. Chilton, The manufacture of nitric acid by the oxidation of ammoniaChemical Engineering Progress Monograph Series No. 3, vol. 56, American Institute of Chemical Engineers, New York, 1960.
[2] C.W. Nutt, S.W. Kapur, Nature 220 (1968) 697; C.W. Nutt, S.W. Kapur, Nature 224 (1969) 169.
[3] Y.M. Fogel, B.T. Nadykto, V.G. Rybalko, V.I. Shvachko, I.E. Korebehanskaya, Kinet. Catal. 5 (1964) 169.
[4] T. Pignet, L.D. Schmidt, J. Catal. 40 (1975) 212.
[5] V.V. Barelko, Yu.E. Volodin, Dokl. Akad. Nauk SSSR 211 (1973) 1373.
[6] B.A. Morrow, I.A. Cody, J. Catal. 45 (1976) 151.
[7] J.J. Ostermaier, J.R. Katzer, W.H. Manogue, J. Catal. 33 (1974) 457.
[8] E.V. Rebrov, M.H.J.M. de Croon, J.C. Schouten, Chem. Eng. J. 90 (2002) 61.
[9] J.L. Gland, V.N. Korchak, J. Catal. 53 (1978) 9.
[10] M. Asscher, W.L. Guthrie, T.-H. Lin, G.A. Somorjai, J. Phys. Chem. 88 (1984) 3233.
[11] D.S.Y. Hsu, D.W. Squire, M.C. Liu, J. Chem. Phys. 89 (1988) 2861.
[12] W.D. Michev, W. Ho, Surf. Sci. 322 (1995) 151.
[13] J.M. Bradley, A. Hopkinson, D.A. King, J. Phys. Chem. 99 (1995) 17032.
[14] M. Kim, S.J. Pratt, D.A. King, J. Am. Chem. Soc. 122 (2000) 2409.
[15] A. Scheibe, S. Günther, R. Imbihl, Catal. Lett. 86 (2003) 33.
[16] M. Flytzani-Stephanopoulos, S. Wong, L.D. Schmidt, J. Catal. 49 (1977) 51.
[17] M. Flytzani-Stephanopoulos, L.D. Schmidt, Prog. Surf. Sci. 9 (1979) 83.
[18] R. McCabe, T. Pignet, L.D. Schmidt, J. Catal. 32 (1974) 114.
[19] M.R. Lyubovsky, V.V. Barelko, J. Catal. 149 (1994) 23.
[20] T.C. Wei, J. Phillips, Adv. Catal. 41 (1992) 359.
[21] A. Winkler, X. Guo, H.R. Siddiqui, P.L. Hagans, J.T. Yates, Surf. Sci. 201 (1988) 419.
[22] C.T. Campbell, G. Ertl, H. Kuipers, J. Segner, J. Chem. Phys. 73 (1980) 5862.
[23] R.J. Gorte, L.D. Schmidt, J.L. Gland, Surf. Sci. 109 (1981) 367.
[24] J.M. Gohndrone, R.I. Masel, Surf. Sci. 209 (1989) 44.
[25] R. Imbihl, Mod. Phys. Lett. B 6 (1992) 493.
[26] S. Ladas, R. Imbihl, G. Ertl, Surf. Sci. 197 (1988) 153; J. Falta, R. Imbihl, M. Henzler, Phys. Rev. Lett. 64 (1990) 1409.

[27] A. Fahmi, R.A. van Santen, Z. Phys. Chem. 197 (1996) 203;
W. Offermans, R.H. van Santen, in preparation.
[28] A. Scheibe, M. Hinz, R. Imbihl, Surf. Sci., submitted for publication.
[29] D.W. Blakely, G.A. Somorjai, Surf. Sci. 65 (1977) 419.
[30] D.P. Sobczyk, A.M. de Jong, E.J.M. Hansen, R.A. van Santen, J. Catal. 219 (2003) 156.
[31] M. Flytzani-Stephanopoulos, L.D. Schmidt, R. Caretta, J. Catal. 64 (1980) 346.
[32] C.G. Takoudis, L.D. Schmidt, J. Catal. 84 (1983) 235.
[33] M. Sheintuch, J. Schmidt, J. Phys. Chem. 92 (1988) 3404.
[34] L. Lobban, G. Philippou, D. Luss, J. Phys. Chem. 93 (1989) 733.
[35] Q. Ge, M. Neurock, JACS 126 (2004) 1551.
[36] V.A. Kondratenko, M. Baerns, J. Catal., submitted for publication.
[37] A. Scheibe, Thesis, Hannover, 2003.
[38] S.M. Davis, F. Zaera, G.A. Somorjai, J. Catal. 77 (1982) 439;
S.M. Davis, F. Zaera, G.A. Somorjai, J. Catal. 85 (1984) 206.
[39] J.M. Gohndrone, C.W. Olsen, A.L. Backman, T.R. Gow, E. Yagasaki, R.I. Masel, J. Vac. Sci. Technol. A 7 (1989) 1986.
[40] A.T. Gee, B.E. Hayden, J. Chem. Phys. 113 (2000) 10333.
[41] T. Fink, J.-P. Dath, R. Imbihl, G. Ertl, J. Chem. Phys. 95 (1991) 2109.